In-Plane and Out-of-Plane Mechanical Properties of Zero Poisson's Ratio Cellular Structures for Morphing Application

SONG Leipeng[1], LI Qiang[2], WANG Hongjie[1], WANG Taoxi[1], NIE Xiaohua[3],*
KONG Xiangsen[1], SHEN Xing[1]

1. State Key Laboratory of Mechanics and Control of Mechanical Structures, Nanjing University of Aeronautics and Astronautics, Nanjing 210016, P. R. China;
2. Beijing Institute of Space Long March Vehicle, Beijing 100048, P. R. China;
3. Computational Structure Technique & Simulation Center, Aircraft Strength Research Institute of China, Xi'an 710065, P. R. China

Abstract: Intelligent structures like zero Poisson's ratio (ZPR) cellular structures have been widely applied to the engineering fields such as morphing wings in recent decades, owing to their outstanding characteristics including light weight and low effective modulus. In-plane and out-of-plane mechanical properties of ZPR cellular structures are investigated in this paper. A theoretical method for calculating in-plane tensile modulus, in-plane shear modulus and out-of-plane bending modulus of ZPR cellular structures is proposed, and the impacts of the unit cell geometrical configurations on in-plane tensile modulus, in-plane shear modulus and out-of-plane bending modulus are studied systematically based on finite element (FE) simulation. Experimental tests validate the feasibility and effectiveness of the theoretical and FE analysis. And the results show that the in-plane and out-of-plane mechanical properties of ZPR cellular structures can be manipulated by designing cell geometrical parameters.

Key words: cellular structure; zero Poisson's ratio (ZPR); mechanical properties; parameter design; morphing application

0 Introduction

Morphing wings are regarded as a developing direction of aircraft, which can significantly improve the aerodynamic and aeromechanics performance, reduce the fuel consumption and expand the flight envelope, depending on flight missions and conditions[1-4]. The morphing wings system, as a creative concept emerging in aircraft design, is composed by a morphing skin, a uniformly distributed driving system with high power energy density and a control device[5-6]. The most important characteristics of morphing skin are low in-plane stiffness and high out-of-plane stiffness to bear the aerodynamic load[5,7]. To obtain optimal performance of morphing skin, many scholars have launched thousands of trials various mechanism model. Composite corrugated structures have been proposed for morphing skin panels in trailing edge region of a wing by Thill et al.[8]. After that, the mechanical properties of a series of corrugated sandwich structure have been studied systematically[9-10]. However, the corrugated sandwich structure has strong load bearing capability but usually with heavy weight or low morphing capability. Kikuta[11] investigated the mechanical properties of a type of thermoplastic polyurethanes, copolyester elastomer, shape memory polymer, or woven materials that could be used as a skin for a morphing wing. Unfortunately, those materials remain prob-

lems of brittleness and thermal fatigue.

Honeycomb structures with a favorable balance of properties containing remarkable lightweight and outstanding mechanical properties are fascinating candidates for application in the fields of morphing skin[12-13]. Chen and Chang et al.[14-15] used sandwiched morphing skin consisted of cellular structure and flexible silicone rubber for morphing aircraft. In addition, honeycomb configurations like SILICOMB[16] and re-entrant[17-18] showed a similar characteristics of high morphing capability and low weight. Among these previous experiments, when honeycombs with positive Poisson's ratio and negative Poisson's ratio are bearing the out-of-plane aerodynamic loads, the inherent anticlastic and synclastic curvature would appear, which is a key challenge for their application in morphing wings[19-20]. However, the zero Poisson's ratio (ZPR) feature can preclude significant increase of effective stiffness in horizontal direction by limiting the contraction (or bulging) in vertical direction[21-22]. Honeycombs with ZPR feature present no contraction in vertical direction when loaded along the wingspan, which exactly satisfies the requirements of the application of morphing wings.

The majority of honeycomb structures proposed in previous studies were suitable for one-dimensional uniaxial morphing or two-dimensional shear morphing. The in-plane properties of conventional hexagonal cellular structures were investigated by Gibson and Ashby et al.[23]. Applying finite element (FE) homogenization, Huang et al.[24] found that the thickness and the corner radius of cell wall would affect the elastic properties of two types of honeycomb with ZPR. Gong et al.[25] investigated a honeycomb with four-angle star-shaped cells that can achieve deformations along two orthogonal directions. Similarly, in Liu's reports[26-27], the in-plane equivalent elastic modulus of ZPR hybrid and accordion cellular structure was deduced detail. However, the calculation methods of out-of-plane equivalent elastic modulus were not given in those reports. In fact, the camber is the most fundamental and crucial factor for wings to generate lift. Changing the camber trailing edge can effectively change the airflow separation on the wing surface and signif-

icantly improve the flight mobility of the aircraft, especially for low-speed aircraft that are usually in low Reynolds number flight conditions and whose performance mainly depends on laminar boundary layer flow.

To meet requirements of mechanical performance of morphing wings undergoing complicated working condition, it is necessary to clarify the in-plane and out-of-plane mechanical properties of honeycomb structures. In this work, in-plane and out-of-plane mechanical properties of ZPR cellular structures are investigated through a combination of theoretical analysis and FE homogenization. The parameters analysis is performed to describe the impacts of the unit cell geometrical configurations on the in-plane and out-of-plane mechanical properties of ZPR cellular structures. Finally, a series of experiments are carried out to validate the feasibility and effectiveness of the theoretical and FE analysis.

1   Model and Experiment Tests

1.1   Analytical models

Fig.1(a) shows the schematic diagram of the honeycomb with ZPR, where the direction-1 and direction-2 represent transverse and vertical direction, respectively. During the deformation analysis process, the unit cell of the honeycombs is regarded a homogeneous plate with effective modulus owing to the cyclic substructure[28], as illustrated in the red marked area. Fig.1(b) shows the geometric parameters of the unit cell with internal angles θ, where l represents the length of inclined wall, $h=2\alpha l$ the length of vertical walls, $t=\beta l$ the thickness of the hexagon, and b the thickness of whole honeycombs perpendicular to 1-2 plane. Here, α and β represent the aspect ratio and cell wall thickness ratio, respectively.

Obviously, the large tensile deformation along direction-2 cannot be achieved in the proposed cellular structure, so that this study considered only areas regarding the in-plane tensile modulus along direction-1. In order to calculate the in-plane tensile modulus along direction-1, a unit cell structure is selected, and its analytical model is shown in Fig.2(a).
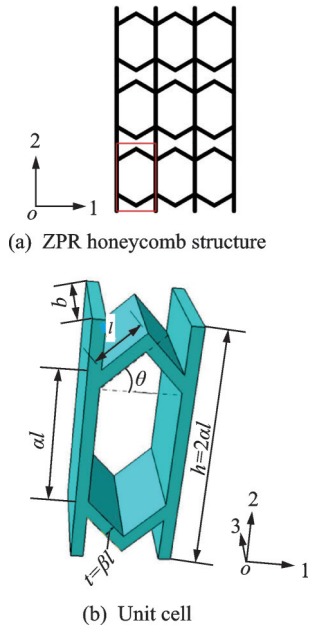
(a) ZPR honeycomb structure

(b) Unit cell

Fig.1　Schematic diagram of the honeycomb with ZPR

(a) Tensile stress along direction-1

(b) Simplified model

Fig.2　Analytical model used to calculate the in-plane tensile modulus

The first step for model is simplification as shown in Fig.2(b), which transforms the model into a quarter model owing to the biaxial symmetry. After simplification, the fixed boundary is set to the left end of the model, while the right is set with a concentrated force F and a moment M. On one hand, the deformation of the honeycombs with ZPR is mostly driven by the bending of the inclined walls when honeycombs withstand a load along direction-1[29]. One the other hand, the length of the vertical wall along direction-1 is small than that of the inclined walls. Therefore, the tensile deformation of the vertical honeycomb wall is ignored, and only the bending and tensile deformation of the cellular structure is considered in this paper.

According to the equilibrium equations, it can be concluded that the vertical force is zero, and the moment M is

$$M = \frac{1}{2} F l \sin \theta \qquad (1)$$

The strain energy U of a cantilever beam subjected to bending moment $M(x)$ and axial load $F_N(x)$ can be expressed as

$$U = \int_0^l \frac{M^2(x)}{2EI} \mathrm{d}x + \int_0^l \frac{F_N^2(x)}{2EA} \mathrm{d}x \qquad (2)$$

where E, I and A are the Young's modulus, inertia moment and cross sectional area, respectively.
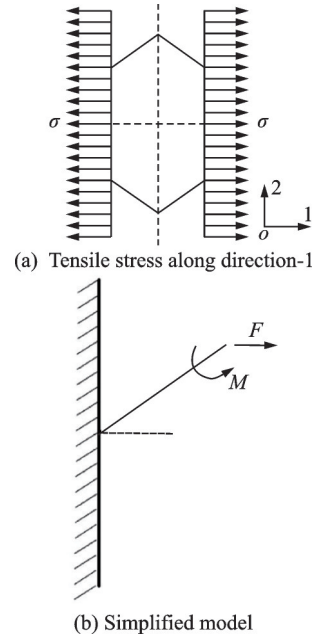
In this paper, it is assumed that bending mo-

ment in the anti-clockwise direction is positive. By now the bending moment is

$$M(x) = \left(\frac{1}{2} l - x\right) F \sin \theta \qquad (3)$$

And the axial load is

$$F_N(x) = F \cos \theta \qquad (4)$$

Substituting Eqs.(3) and (4) into Eq.(2), it can be concluded that the strain energy U is

$$U = \frac{F^2 l^3 \sin^2\theta}{24 E_s I} + \frac{F^2 l \cos^2\theta}{2 E_s A} \qquad (5)$$

where E_s is the Young's modulus of raw materials.

According to the Castigliano's second theorem[30], when the elastic system is enduring static load, the displacement δ_i of the point of force action can be calculated by the partial derivative of the strain energy U with respect to any applied force F_i, shown as

$$\delta_i = \frac{\partial U}{\partial F_i} \qquad (6)$$

Combining Eq.(5) and Eq.(6), it can be concluded that horizontal displacement of the point of force action is

$$\delta_1 = \frac{F l^3 \sin^2\theta}{12 E_s I} + \frac{F l \cos^2\theta}{E_s A} \qquad (7)$$

According to the homogenization theory, the equivalent tensile modulus E_1 can be deduced by the equivalent stress σ_1 and strain ε_1 that

$$\sigma_1 = \frac{F}{\alpha l b} \tag{8}$$

$$\varepsilon_1 = \frac{\delta_1}{l \cos \theta} \tag{9}$$

$$E_1 = \frac{\sigma_1}{\varepsilon_1} \tag{10}$$

Substituting Eqs.(7—9) into Eq.(10), it can be concluded that the homogenized and dimensionless tensile modulus can be expressed as

$$\frac{E_1}{E_s} = \frac{\beta^3 \cos \theta}{\alpha(\sin^2\theta + \beta^2 \cos^2\theta)} \tag{11}$$

It is most important to research the equivalent shear modulus of the proposed cellular structures for application of flexible skin undergoing sweep morphing. Fig.3 shows the schematics of unit cell model used to calculate the equivalent shear modules. The fixed boundary is set to the left end of the model, while the right is set with a concentrated force F along direction-2 and a moment M along direction-1.
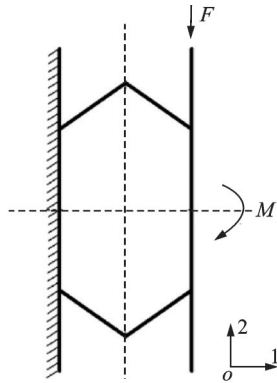

Fig.3   Schematics of unit cell model used to calculate the equivalent shear modules

According to the equilibrium equations, it can be concluded that the moment M is zero, and F is

$$F = \tau b \alpha l \tag{12}$$

And the vertical deformation induced by shear force can been obtained according to Euler-Bernoulli theory[31]

$$\delta_2 = \frac{2\omega F l^3}{E_s I} \cos^2\theta \tag{13}$$

where

$$\omega = \frac{4}{3} - \frac{12(\alpha + \sin\theta)^2}{\alpha^3 + 12\alpha^2 + 24\alpha\sin\theta + 16\sin^2\theta} \tag{14}$$

It can be concluded that the shear strain is

$$\gamma = \frac{\delta_2}{2l \cos \theta} \tag{15}$$

According to the definition of shear modulus, the homogenized and dimensionless shear modulus can be expressed as

$$\frac{E_2}{E_s} = \frac{\beta^3}{12\alpha\omega \cos \theta} \tag{16}$$

where E_2 is the equivalent shear modulus of the ZPR cellular structures.

For a cellular structure, which is designed for a wing with a variable camber trailing edge, it is essential to understand the bending deformation. According to the Chen's report[32], the calculation method for in-plane Young's modulus of honeycomb cell was inapplicable to out-of-plane bending modulus since the moment acting on inclined walls are different for in-plane deformation and bending deformation. Fig.4(a) shows the loading scheme of the honeycomb cell. After simplification, the theoretical model in Fig.4(a) has been transformed into an 1/4 model, as shown in Fig.4(b), owing to the biaxial symmetry. The deformation of the vertical honeycomb wall is ignored.
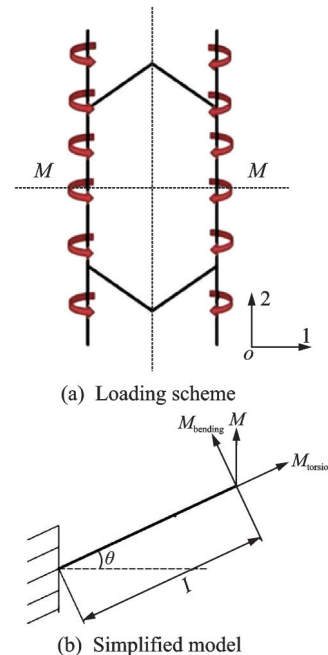

(a) Loading scheme

(b) Simplified model

Fig.4   Analytical model used to calculate the out-of-plane bending modulus

The moment M is divided into two parts, namely bending moment $M_{bending}$ and torsional moment $M_{torsion}$, shown as

$$M_{bending} = M \cos \theta \tag{17}$$

$$M_{torsion} = M \sin \theta \tag{18}$$

Then the bending angle around the direction-1 induced by $M_{bending}$ can be obtained

$$\theta_{bending} = \frac{M_{bending}l}{E_s I} \cos\theta \qquad (19)$$

Different from the torsion of a bar with circular section, the plane assumption is no longer applicable to the torsion of a bar with rectangular section. In fact, after the torsion deformation occurs, the lateral circumferential boundary of a bar with rectangular section becomes a spatial curve. For a bar with rectangular section, the normal stress caused by the constrained torsion is very small, resulting in that the constrained torsion is no different from the natural torsion. A theoretical formula of the bending angle around the direction-1 induced by $M_{torsion}$ is proposed that

$$\theta_{torsion} = q\frac{M_{torsion}l}{KG_s}\sin\theta \qquad (20)$$

where q is the torsion coefficient, $G_s = \dfrac{E_s}{2(1+\nu)}$ the shear modulus of the based materials, and K the Polar moment of inertia of solid rectangular section[28] and can be calculated by

$$K = \frac{1}{16}b(\beta l)^3\left[\frac{16}{3} - 3.36\frac{\beta l}{b}\left(1 - \frac{(\beta l)^4}{12b^4}\right)\right] \qquad (21)$$

The torsion coefficient q of a bar with rectangular section has been detailed in the Huang's investigation[33].

Replace E_s with the Kirchhoff plate formula $\dfrac{E_s}{1-\nu^2}$ to calculate the out-of-plane bending modulus of the beam in a relatively large width and thus one can obtain the equivalent out-of-plane bending modulus of the proposed honeycomb cell as

$$E_b = \frac{Ml\cos\theta}{\frac{1}{1-\nu^2}\theta_b I_b} \qquad (22)$$

where ν and $I_b = \dfrac{\alpha lb^3}{12}$ are the Poisson's ratio and the second moment of cross sectional area of the beam, respectively.

The total angular deformation of the structure around the direction-1 can be calculated as

$$\theta = \theta_{bending} + \theta_{torsion} \qquad (23)$$

Apparently, combining Eqs.(17—23), the ho-

mogenized and dimensionless bending modulus can be calculated by the following form

$$\frac{E_b}{E_s} = \frac{12\beta(1-\nu^2)K\cos\theta}{\alpha(12K\cos^2\theta + 2(1+\nu)\beta lb^3 q\sin^2\theta)} \qquad (24)$$

1.2 FE homogenization

In order to verify the calculation results in theory, the numerical simulation with a commercial FE software ABAQUS (version 6.14) was carried out. The material selected to perform the simulation was photosensitive resin with the elasticity modulus of 2 800 MPa, and the Poisson's ratio of 0.33. Internal geometric parameter of $l=10$ mm is adopted. The simulation was carried out with aspect ratio α (2, 2.5 and 3), cell wall thickness ratio β (0.1, 0.15, 0.2) and cell angle θ ranged from $-45°$ to $45°$ with even step at $5°$.

Fig.5 shows the FE model used to calculate the in-plane tensile modulus of honeycombs with ZPR. In the model, a 2-node linear element B21 is used to model the honeycomb block. The boundary conditions with fixed surface A and loaded surface B are shown in Fig.5. For the tensile deformation, the surface B was loaded with 10 kN uniform load along direction-X. Accordingly, the surface B was loaded with 10 kN uniform load along direction-Y for shear deformation.
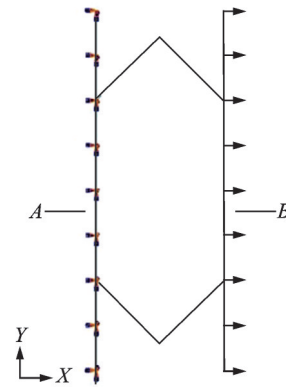

Fig.5 FE model used to calculate the in-plane mechanics of honeycombs with ZPR

As shown in Fig.6, 3D model with 3×6 unit cells was employed to calculate the out-of-plane bending modulus. Mesh convergence results show that the model with a minimum element size of $t/2$ can obtain accurate results. In the model, an 8-node

linear brick C3D8R is used to model the honeycomb block. As for the boundary conditions, surface A was constrained and surface B was loaded with 10 kN concentrated force along direction-Z in the form of coupling. And the rest of surfaces was set as free boundary. Then the equivalent bending modulus can be calculated by the following form

$$E_b = \frac{Fl^3}{3wI_b} \tag{25}$$

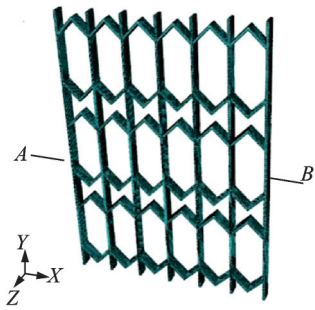where w is the deflection of the structure along the direction-Z.

Fig.6   FE model used to calculate the out-of-plane mechanics of honeycomb with ZPR

1. 3   Manufacturing and experiment tests

As the honeycomb structure is complex, it is difficult to machine them by traditional technology. Thus, the state-of-the-art additive layer manufacturing technology is utilized to prepare the cellular structure with ZPR, which makes it possible to evaluate the mechanical performance of structure in a convenient and cost-efficient way. All honeycomb samples employed in this investigation were fabricated using a Stereolithography (SLA) machine (3DSL-360Hi, Shanghai Digital Electronics Technology Co., Ltd, China) with photosensitive resin (PS). The manufactured precision of the test specimen is highly dependent on the machine type and the minimum thickness dimension of the printed structure is restricted to 1 mm with 200 μm precision. Firstly, the designed model of honeycomb panel was imported as ".stl" file and then sliced by the printing software. Then, the honeycomb panel was built layer-by-layer with a layer thickness of 50 μm through a down-top printing process. After cleaning off the uncured photosensitive resin off the surface, the printed honeycombs were put in an oven to go through drying process. The geometric average val-

ue of the Young's modulus of the PS, SZUV-W8001, is 2 800 MPa.

The in-plane and out-of-plane mechanical properties of the proposed ZPR cellular structures were conducted on former testing machine with a constant displacement rate of 1 mm/s. Corresponding force and displacement during tests were recorded to calculate the tensile modulus, shear modulus and bending modulus of ZPR cellular structures. For the test of homogenized tensile modulus, the ZPR cellular structure specimens had dimensions of 130 mm× 120 mm×5 mm, and load transmitting blocks with appropriate width were designed in tensile specimens to prefer the standards ASTM D638-08[34]. A method used for calculating shear modulus was different from off-axial test. Specimen with unit cell had dimensions of 40 mm×15 mm×5 mm, as illustrated in Fig.7. Ears to fit the grip was designed, via which the shear forces could be transmitted to the corresponding edges of unit cells so that the effective shear modulus of unit cells could be both obtained under axial movement[35]. In addition, a three-point bending tests were carried out to measure the out-of-plane bending performance of the honeycomb with dimensions of 100 mm×120 mm×5 mm. A constant displacement rate of 5 mm/min and a span length of 80 mm were used during three-point bending test.
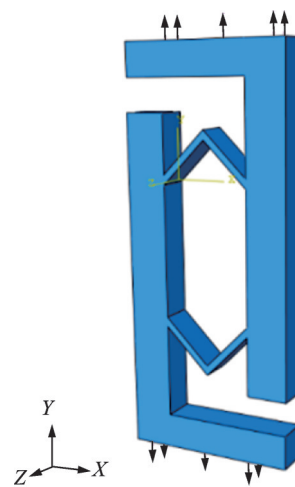

Fig.7   Schematic of shear tested specimen

2   Results and Discussion

2. 1   Parametric analysis

From Eqs.(11, 16, 24), one can make predictions and calculations of the in-plane and out-of-

plane mechanics of ZPR cellular structures based on the geometric parameters including α, β and θ. Fig.8 shows the comparison of FE results and theoretical results for the dimensionless equivalent elastic modulus E_1/E_s of the proposed ZPR cellular structures varying with the geometric parameters. The results show that the in-plane stiffness of the proposed ZPR cellular structures in this investigation resembles the Gibson-Ashby model owing to the similar hexagonal geometrical configurations[23]. However, in the Rubert's analytical model[36], the ZPR cellular structures were identified as only undergoing pure bending, resulting that the transverse stiffness approach infinity at $\theta=0°$, which are not agree with practice situation. After taking axial deformation of cell walls into consideration, in-plane tensile modulus of the ZPR cellular structures no longer be infinity at $\theta=0°$ in this study. As shown in Figs.8, 9, the analytical results of the dimensionless equivalent elastic modulus of ZPR cellular structures are consistent with the FE results, and the average relative error is around 3%. Making a general survey of the overall situation at the same time, the maximum error is 7.5% occur-

Fig.8   FE and analytical results of E_1/E_s of the ZPR cellular structure versus cell angle

ring at $\alpha=3$, $\beta=0.15$ and $\theta=35°$ between analytical result and FE simulation.

As shown in Fig.8(a), E_1/E_s reaches its extreme value at $\theta=0°$ firstly, and at this point, inclined walls in horizontal direction undergo the pure tensile, leading to a maximum E_1/E_s value. Second, E_1/E_s has a symmetric distribution centered on $\theta=0°$ when α and β are definite values. If $\theta>0°$ is taken alone, E_1/E_s decreases as the cell angle θ increases. Finally, E_1/E_s increases with the increasing of the parameter β when other parameters remain constant. Similarly to Fig.8(a), E_1/E_s reaches its extreme value at $\theta=0°$ and has a normal distribution centered on $\theta=0°$ when parameters α and β remain constant in Fig.8(b). When $\theta>0°$, E_1/E_s decreases as the cell angle θ increases. In addition, E_1/E_s decreases with the increasing of the parameter α when other parameters remain constant owing to the increased cross-sectional area induced by the parameters α. Comparing Fig.8(a) and Fig.8(b), the variations of parameter α produce smaller fluctuations on E_1/E_s than the variations of parameter β do. The variations of E_1/E_s values are of the same order of magnitude when α ranges from 2 to 3, while the increment value of E_1/E_s ranges from one order of magnitude to two orders of magnitude when β ranged from 0.1 to 0.2. It gives a good reference model for the designs of the in-plane elastic modulus by various parameter β.

Fig.9 shows the comparison of FE results and theoretical results for the dimensionless equivalent shear modulus E_2/E_s of ZPR cellular structures varying with the geometric parameters. The analytical results of the dimensionless equivalent shear modulus E_2/E_s of ZPR cellular structures are also consistent with the FE results. And the mean relative deviations of E_2/E_s of ZPR cellular structures between analytical results and FE results are less than 3%, while the max deviation is 7% occurring at $\alpha=2$, $\beta=0.2$ and $\theta=45°$. Unlike the dimensionless equivalent elastic modulus E_1/E_s, the dimensionless equivalent shear modulus E_2/E_s is not symmetrically distributed. E_2/E_s firstly decreases, then increases with the increasing of cell angle θ from $-45°$ to $45°$ when α and β are definite values. In addition, the
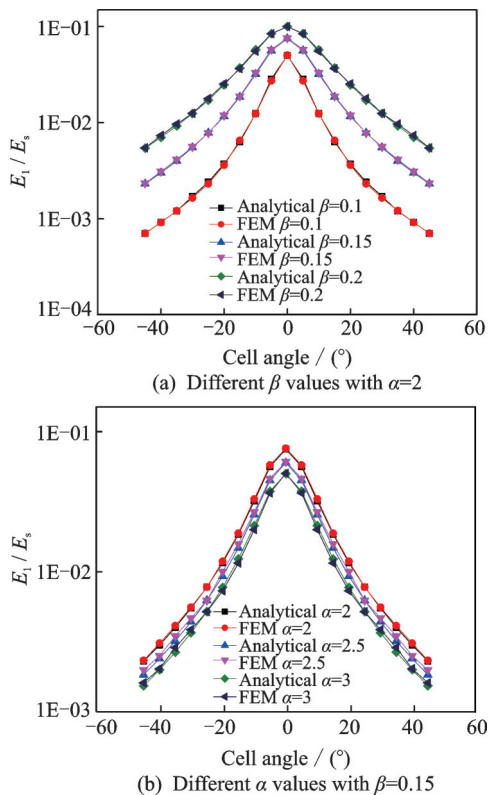
minimum values of E_2/E_s are concerned with the geometric parameters of the unit cell. The FE results, it should be noted, are somewhat below the analytical ones, which is contributed by the difference between FE model and theoretical model[37]. In fact, the beam model applied to the FE simulation is the Timoshenko beam, while to theoretical analysis is the Euler-Bernoulli beam. As shown in Fig.9(a), E_2/E_s increases with the increasing of the parameter β when other parameters are definite values. It can be found in Fig.9(b) that the increase of the parameter α leads to a decrease of dimensionless equivalent shear modulus when other parameters remain constant.

(a) Different β values with $\alpha=2$

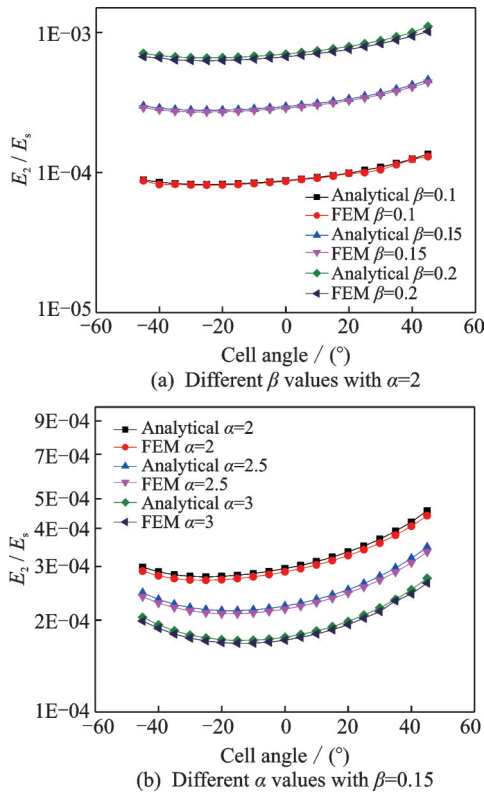(b) Different α values with $\beta=0.15$

Fig.9　FE and analytical results of E_2/E_s of the ZPR cellular structure versus cell angle

Fig.10 shows the comparison of FE results and theoretical results for the dimensionless equivalent bending modulus E_b/E_s of ZPR cellular structures varying with the geometric parameters. The analytical results of the dimensionless equivalent bending modulus E_b/E_s of ZPR cellular structures are also consistent with the FE results. And the mean relative deviations of E_b/E_s of ZPR cellular structures between analytical results and FE results are less than 20%, while the max deviation is 35% occurring at $\alpha=2$, $\beta=0.2$ and $\theta=0°$. In addition, the de-

viations between analytical results and FE results decrease with the cell angle θ increases when $\theta>0°$. Both in Fig.10(a) and Fig.10(b), E_b/E_s reaches its extreme value at $\theta=0°$, and at this point, inclined walls in horizontal direction undergo the pure bending, leading to a maximum E_b/E_s value. When α and β are definite values, E_b/E_s has a symmetric distribution centered on $\theta=0°$. If you take $\theta>0°$ alone, an increasing cell angle θ leads to a decrease of E_b/E_s. In addition, the out-of-plane bending modulus increases with increasing of the parameter β, while decreases with increasing of the parameter α, which is similar to what observed by Huang et al.[34]. From these simulations it is apparent that the simplifying assumption for the analytical model (i.e., neglecting the deformation of the vertical wall) leads to discrepancies against the higher fidelity FE model. The deformation of the vertical wall versus the whole cell deformation increases for increasing dimensions of the vertical wall. An increase of the cell wall aspect ratio not only leads to a slightly decrease of the equivalent bending modulus, but also leads to a relatively larger discrepancy between the analytical and the FE results.
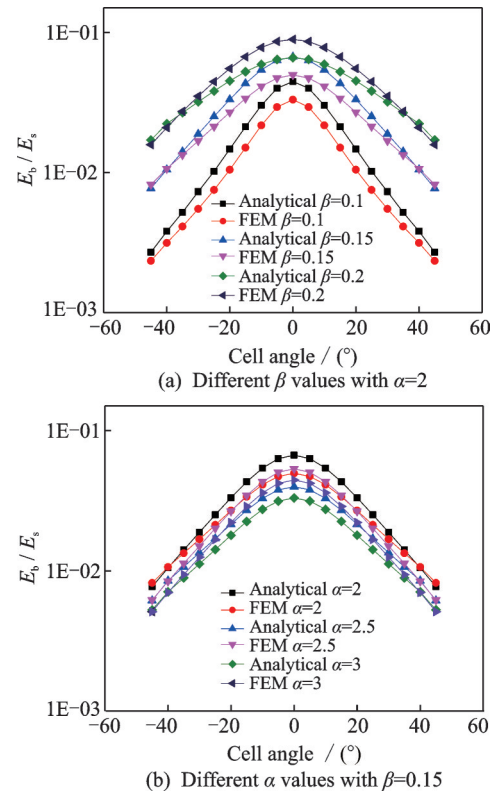

(a) Different β values with $\alpha=2$

(b) Different α values with $\beta=0.15$

Fig.10　FE and analytical results of E_b/E_s of the ZPR cellular structure versus cell angle

2. 2   Experiment results

To verify the correctness of previous analytical and FE results, honeycomb specimens with $l=10$, $\alpha=2$, $\beta=0.1$ and $\theta=45°$ were used in experimental test for in-plane and out-of-plane mechanics. Fig.11 shows the tensile, shear and bending mechanical properties of the honeycomb with ZPR. Then the corresponding equivalent tensile moduli, equivalent shear moduli and equivalent bending moduli are calculated and listed in Table 1. In addition, the analytical and FE results are also listed in Table 1 to make a comparison with experimental results. For the equivalent tensile modulus E_1, the deviation between experimental and analytical results is 1.02%,
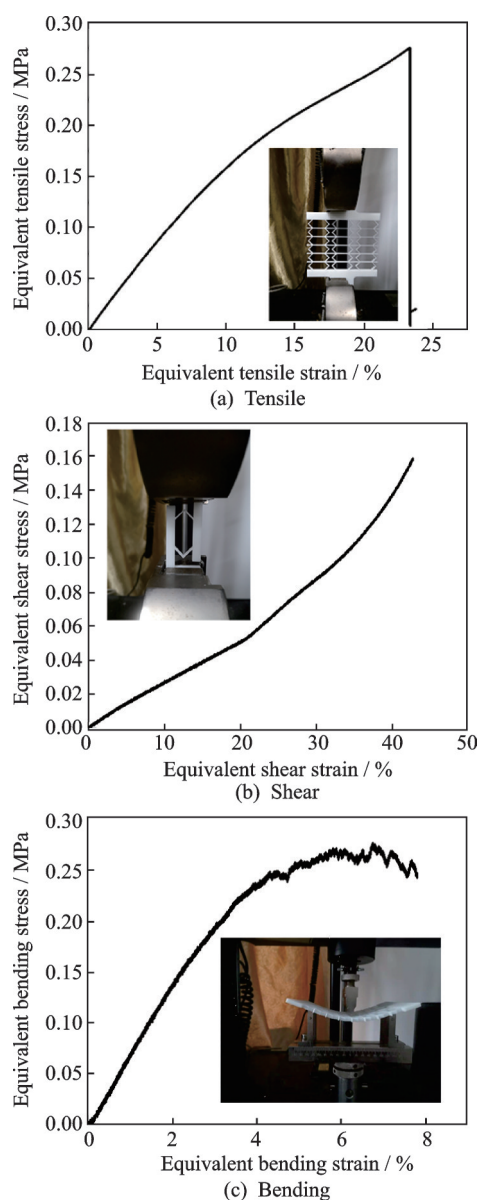
and the deviation between experimental and FE results is 1.52%. For the equivalent shear modulus E_2, the experimental results show discrepancies between 5.26% and 1.05% over the analytical and FE results, respectively. In addition, for the equivalent bending modulus E_b, the deviation between experimental and analytical results is 12.03%, and the deviation between experimental and FE results is 15.27%. Those discrepancies between the analytical, FE and experimental results can be attributed to several reasons. First, the SLA is very similar to fusion deposition molding, both having a layerwise deposition and an additional degree of internal porosity that do not meet the assumption of a homogeneous and isotropic honeycomb materials[38]. Second, in the tensile, shear and bending theoretical models, the deformation of the vertical honeycomb wall is ignored. In addition, even when the fixture produces a pure shear deformation as closely to the ideal case, there are still differences between a pure shear deformation and an approximate one[39]. As shown in Table 1, for whether in-plane or out-of-plane mechanical properties, the deviation between experimental data and numerical prediction is less than 2%.

Table 1   Comparison of the analytical, FEM, and experiment results   MPa

Parameter	Analytical	FEM	Experiment
E_1	1.96	1.97	1.94±0.12
E_2	0.38	0.36	0.36±0.03
E_b	7.56	6.55	6.65±0.15

3   Conclusions

Analytical models are established for the calculation of in-plane and out-of-plane mechanical properties of ZPR cellular structures in combination with the FE analysis. The experimental test validates correctness and effectiveness of the theoretical and FE analysis. According to the parametric analysis, these cell geometric parameters provide different contributions to the effective mechanical properties and lead to a separate design for the in-plane and out-of-plane performances. Therefore, the superior technique could be an efficient reference to mechanic engineering such as morphing aircraft design. For

Fig.11   Mechanical properties of the honeycomb with ZPR

example, a large cell angle θ of inclined wall and a large aspect ratio α could be employed for one dimensional morphing. And the variations of aspect ratio produce smaller fluctuations on the dimensionless equivalent elastic modulus than the variations of the thickness of inclined wall. To obtain the better shear morphing, ZPR cellular structures with large aspect ratio α and lower cell angle θ could be selected. Aimed at some complex flight conditions, the multi-objective optimization could be performed with a comprehensive consideration of the in-plane and out-of-plane mechanics of ZPR cellular structures. However, this work still has some weaknesses and drawbacks. The results, both analytical and experimental, presented so far do not consider the effects of geometric and material nonlinearities. Hence, they are only applicable for small deformations and not accurate when the honeycomb cores present large local strains or material plastic behaviors. In future work, the mechanical properties of the ZPR honeycomb structure should be explored by considering the nonlinear behavior of honeycomb under large deformation.

References

[1]   JOSHI S, TIDWELL Z W, CROSSLE Y, et al. Comparison of morphing wing strategies based upon aircraft performance impacts[C]//Proceedings of the 45th AIAA/ASME/ASCE/AHS/ASC Structures, Structural Dynamics & Materials Conference. Palm Springs, California: AIAA, 2004.

[2]   AFONSO F, VALE J, LAU F, et al. Performance based multidisciplinary design optimization of morphing aircraft[J]. Aerospace Science and Technology, 2017, 67: 1-12.

[3]   LI W C, JIN D P. Gain-scheduled control and stability analysis of morphing aircraft in transition process[J]. Transactions of Nanjing University of Aeronautics and Astronautics, 2018, 35(6): 1080-1086.

[4]   ZHANG X Y, LI Y, LI J F, et al. Prediction of compressive and shear moduli of X-cor sandwich structures for aeronautic engineering[J]. Transactions of Nanjing University of Aeronautics and Astronautics, 2015, 32(6): 646-653.

[5]   GANDHI F, ANUSONTI-INTHRA P. Skin design studies for variable camber morphing airfoils[J]. Smart Materials and Structures, 2008, 17: 015025-015033.

[6]   ÖZGEN S, YAMAN Y, ŞAHIN M, et al. Morphing air vehicle concepts[C]//Proceedings of the International Workshop on Unmanned Vehicle[S.l.]: [s.n.], 2010: 46-51.

[7]   AI Sen, GUO Yuchao, NIE Xiaohua, et al. One-dimensional deformation behavior of a honeycomb structure with zero Poisson's ratio[J]. Journal of Nanjing University of Aeronautics and Astronautics, 2021, 53(4): 629-636. (in Chinese)

[8]   THILL C, ETCHES J A, BOND I P, et al. Composite corrugated structures for morphing wing skin applications[J]. Smart Materials and Structures, 2010, 19: 12000912.

[9]   ZHU Y, QIN Q, ZHANG J. On effective mechanical properties of an orthogonal corrugated sandwich structure[J]. Materials & Design, 2021, 201: 109491.

[10]   DEO A, YU W. Equivalent plate properties of composite corrugated structures using mechanics of structure genome[J]. International Journal of Solids and Structures, 2021, 208/209: 262-271.

[11]   KIKUTA M T. Mechanical properties of candidate materials for morphing wings[M]. Petersburg: Virginia Polytechnic Institute and State University, 2003.

[12]   CAI L C, ZHANG D Y, ZHOU S H, et al. Investigation on mechanical properties and equivalent model of aluminum honeycomb sandwich panels[J]. Journal of Materials Engineering and Performance, 2018, 27: 6585-6596.

[13]   WU H X, LIU Y, ZHANG X C, et al. Effects of distribution of microstructure types on the in-plane dynamic crushing of composite honeycomb structures[J]. Journal of Materials Engineering and Performance, 2021, 30: 850-861.

[14]   CHEN J J, SHEN X, LI J F. Zero Poisson's ratio flexible skin for potential two-dimensional wing morphing[J]. Aerospace Science and Technology, 2015, 45: 228-241.

[15]   CHANG L L, SHEN X. Design of cellular based structures in sandwiched morphing skin via topology optimization[J]. Structural and Multidisciplinary Optimization, 2018. DOI: 10.1007/s00158-018-2020-5.

[16]   VIRK K, MONTI A, TREHARD T, et al. SILICOMB PEEK Kirigami cellular structures: Mechanical response and energy dissipation through zero and negative stiffness[J]. Smart Materials and Structures, 2013, 22: 084014.

[17]   YU R, LUO W, YUAN H, et al. Experimental and numerical research on foam filled re-entrant cellular

structure with negative Poisson's ratio[J]. Thin-Walled Structures, 2020, 153: 106679.

[18] KHAN S Z, MUSTAHSAN F, MAHMOUD E R I, et al. A novel modified re-entrant honeycomb structure to enhance the auxetic behavior: Analytical and numerical study by FEA[J]. Materials Today: Proceeding, 2020. DOI: 10.1016/j.matpr.2020.05.083.

[19] MASTERS I, EVANS K. Models for the elastic deformation of honeycombs[J]. Composite Structures, 1996, 35: 403-422.

[20] ANDERSEN G, COWAN D, PICATAK D. Aeroelastic modeling, analysis ana testing of a morphing wing structure[C]//Proceedings of the 48th AIAA/ASME/ASCE/AHS/ASC Structures, Structural Dynamics, and Materials Conference. Honolulu, Hawaii: AIAA, 2007.

[21] OLYMPIO K R, GANDHI F. Zero Poisson's ratio cellular honeycombs for flex skins undergoing one-dimensional morphing[J]. Journal of Intelligent Material Systems and Structures, 2010, 21: 1737-1753.

[22] LAKES R. Foam structures with a negative Poisson's ratio[J]. Science, 1987, 235: 1038-1040.

[23] GIBSON L J, ASHBY M F. Cellular solids: Structures and properties[M]. 2nd ed. Cambridge: Cambridge University Press, 1997.

[24] HUANG J L, LIU W Y, TANG A M. Effects of fine-scale features on the elastic properties of zero Poisson's ratio honeycombs[J]. Materials Science and Engineering B, 2018, 236/237: 95-103.

[25] GONG X B, HUANG J, LIU T J, et al. Zero Poisson's ratio cellular structure for two-dimensional morphing application[J]. Composite Structures, 2015, 134: 384-392.

[26] LIU W D, LI H L, YANG Z D, et al. Mechanics of a novel cellular structure for morphing applications [J]. Aerospace Science and Technology, 2019, 95: 105479.

[27] LIU W D, LI H L, YANG Z D, et al. In-plane mechanics of a novel cellular structure for multiple morphing applications[J]. Composite Structures, 2019, 207: 598-611.

[28] ZHAO Y, GE M, MA W. The effective in-plane elastic properties of hexagonal honeycombs with consideration for geometric nonlinearity[J]. Composite Structures, 2020, 234: 111749.

[29] LAN L, SUN J, HONG F D. et al. Nonlinear constitutive relations of thin-walled honeycomb structure[J]. Mechanics of Materials, 2020, 149: 103556.

[30] YOUNG W C, BUDYNAS R G. Roark's formulas for stress and strain[M]. New York: McGraw-Hill Education, 2002.

[31] SHIGLEY J, MISHKE C, BUDYNAS R G. Mechanical engineering design[M]. New York: McGraw-Hill Education, 2004.

[32] CHEN D H. Bending deformation of honeycomb consisting of regular hexagonal cells[J]. Composite Structures, 2011, 93: 736-746.

[33] HUANG J, ZHANG Q H, SCARPA F, et al. Bending and benchmark of zero Poisson's ratio cellular structures[J]. Composite Structures, 2016, 152: 729-736.

[34] HUANG J, GONG X B, ZHANG Q H, et al. In-plane mechanics of a novel zero Poisson's ratio honeycomb core[J]. Composites Part B—Engineering, 2016, 89: 67-76.

[35] CHANG L L, SHEN S, DAI Y K, et al. Investigation on mechanical properties of topologically optimized cellular structures for sandwiched morphing skins[J]. Composite Structures, 2020, 250: 112555.

[36] BUBERT E A, WOODS B K S, LEE K, et al. Design and fabrication of a passive 1D morphing aircraft skin[J]. Journal of Intelligent Material Systems and Structures, 2010, 21: 1699-1717.

[37] GONG X B, HUANG J, SCARPA F, et al. Zero Poisson's ratio cellular structure for two-dimensional morphing application[J]. Composite Structures, 2015, 134: 384-392.

[38] LIRA C, SCARPA F, TAI Y H, et al. Transverse shear modulus of SILICOMB cellular structures[J]. Composites Science and Technology, 2011, 71: 1236-1241.

[39] SINGER J, AEBOCZ J, WELLER T. Bucking experiments methods in bucking of thin-walled structures [J]. Applied Mechanics Reviews, 2002, 56: B5.

Authors   Dr. **SONG Leipeng** studied in Nanjing University of Aeronautics and Astronautics in 2020. His research focuses on smart materials and structures.

Mr. **NIE Xiaohua** is an engineer at Aircraft Strength Research Institute of China, Computational Structure Technique & Simulation Center, Xi'an. His research focuses on

（Production Editor：ZHANG Huangqun）

用于变体机翼的零泊松比胞状结构面内和面外力学性能

宋雷鹏[1]，李　强[2]，王泓杰[1]，王韬熹[1]，聂小华[3]，孔祥森[1]，沈　星[1]

（1.南京航空航天大学机械结构力学及控制国家重点实验室，南京 210016，中国；2.北京航天长征飞行器研究所，北京 100048，中国；3.中国飞机强度研究所计算结构技术与仿真中心，西安 710065，中国）

摘要：零泊松比（Zero Poisson's ratio, ZPR）胞状结构等智能结构因其重量轻、有效模量低的突出特点，在变形翼等领域的应用逐渐兴起。本文研究了 ZPR 胞状结构的面内和面外力学性能，提出了计算 ZPR 胞状结构的面内拉伸模量、面内剪切模量和面外弯曲模量的理论方法，分析了蜂窝结构几何构型对其面内、面外力学性能的影响。在有限元模拟的基础上，系统地研究了面内拉伸、剪切模量和面外弯曲模量。实验验证了理论分析和有限元分析的可行性和有效性。结果同时表明，通过设计胞体几何参数可以控制 ZPR 胞状结构的面内和面外力学。

关键词：胞状结构；零泊松比；力学性能；参数设计；变体机翼